https://doi.org/10.5194/gmd-2020-33
Preprint. Discussion started: 27 April 2020


Geoscientific Model Development Discussions

# HIRM v1.0: A hybrid impulse response model for climate modeling and uncertainty analyses

Kalyn Dorheim [1], Steven Smith [1], Ben Bond-Lamberty[1]

[1] Joint Global Change Research Institute, Pacific Northwest National Laboratory, College Park, MD 20740, United States of America

*Correspondence to*: Kalyn Dorheim (kalyn.dorheim@pnnl.gov)

**Abstract.** Simple climate models (SCMs) are frequently used in research and decision-making communities because of their flexibility, tractability, and low computational cost. SCMs can be idealized, flexibly representing major climate dynamics as impulse response functions, or process-based, using explicit equations to model possibly nonlinear climate and earth system dynamics. Each of these approaches has strengths and limitations. Here we present and test a hybrid impulse response modeling framework (HIRM) that combines the strengths of process-based SCMs in an idealized impulse response model, with HIRM's input derived from the output of a process-based model. This structure allows it to capture the crucial nonlinear dynamics frequently encountered in going from greenhouse gas emissions to atmospheric concentration to radiative forcing to climate change. As a test, the HIRM framework was configured to emulate total temperature of the simple climate model Hector 2.0 under the four Representative Concentration Pathways and the temperature response of an abrupt four times $CO_2$ concentration step. HIRM was able to reproduce near-term and long-term Hector global temperature with a high degree of fidelity. Additionally, we conducted two case studies to demonstrate potential applications for this hybrid model: examining the effect of aerosol forcing uncertainty on global temperature, and incorporating more process-based representations of black carbon into a SCM. The open-source HIRM framework has a range of applications including complex climate model emulation, uncertainty analyses of radiative forcing, attribution studies, and climate model development.

## 1 Introduction

Climate models encompass a diverse collection of approaches to representing Earth system processes at various levels of complexity and resolution. The most complex are the Earth System Models (ESMs): highly detailed representations of the physical, chemical, and biological processes governing the Earth system at high spatial and temporal resolution (Hurrell et al. 2013). These models are computationally expensive and therefore can only be run for a limited number of scenarios. Less complex climate models, Simplified Climate Models (SCMs), sacrifice process realism with the benefit that they are computationally inexpensive (van Vuuren et al., 2011). Although SCMs are generally low resolution in space and time, they have a wide range of applications including but not limited to emulation (Dorheim et al. 2019); probabilistic estimates

https://doi.org/10.5194/gmd-2020-33
Preprint. Discussion started: 27 April 2020


Geoscientific Model Development Discussions

demanding thousands of separate model runs (Stainforth et al. 2005; Webster 2012); factor separation analysis (Mheel et al. 2007); and Earth system model development and diagnosis (Meinhausen et al., 2011).

SCMs can be characterized as either process-based or idealized climate models. Process-based SCMs consist of systems of equations that represent, albeit in highly simplified form, carbon cycle and climate dynamics; in contrast, idealized SCMs convolve linear impulse response functions to approximate climate dynamics (Millar et al., 2017). One of the fundamental differences between idealized and process-based SCMs is the representation of the evolution of emissions to climate impacts. Process-based models (whether SCMs or ESMs) have equations that represent emissions accumulating as concentrations, which in turn affect the energy balance at the top of the troposphere (radiative forcing) resulting in climate changes (most prominently, temperature change) (Harvey et al. 1995; Claussen et al. 2002). The system of equations used by process-based SCMs includes nonlinearities such as interactions between atmospheric chemical constituents (Wigley et al. 2002); relationships between greenhouse gas concentrations and energy absorption, i.e. radiative forcing (Shine et al. 1990 and Mhyre et al. 1998); and carbon-climate feedbacks on $CO_2$ concentrations (Wenzel et al. 2014, Tang Riley 2015, and Heinmann and Reichstein 2008).

Idealized SCMs are based on impulse response functions (IRFs) (Aamaas et al., 2013; Fuglestvedt et al., 2003; Millar et al., 2017; Myhre et al., 2013), defined as the system response to a unit perturbation. In the context of climate modeling, the most common IRFs used are temperature responses to emission or concentration perturbations. Models that rely on IRFs, including the impulse response model used in the Intergovernmental Panel on Climate Change Fifth Assessment Report (AR5-IR) (Myhre et al., 2013) use IRFs to represent the time-integrated relationship between emissions and temperature change. In these models, a linear impulse response function is convolved with a time series (Thompson and Randerson 1999). Idealized SCMs have been widely used by the research and decision-making communities (Joos et al. 2013) because they are simple in the sense that they are mathematically transparent, consisting of a small number of equations. Idealized SCMs may exhibit biased results, however, due to their lack of nonlinear dynamics. This can be ameliorated to some extent by adding nonlinear terms to them (Hooß et al. 2001, Millar et al. 2017), although differences from process-based SCMs may still occur (Schwarber et al. 2019). In addition, the physical interpretation of their behavior is not always straightforward.

Here we present a hybrid impulse response modeling framework (HIRM) that uses output from process-based SCMs to incorporate nonlinear dynamics into a linear impulse response model. This framework leverages the nonlinear dynamics of a process-based SCM with the simplicity of an impulse response model. The first two experiments in this paper demonstrate HIRM's ability to accurately reproduce global mean temperature, including the temperature response to large climate system perturbations. We demonstrate the potential utility of this framework in an uncertainty analysis, and by examining how changing the response function for black carbon to reflect recent ESM results impacts HIRM output. The implications of these results are discussed as well as potential future uses of this framework.

https://doi.org/10.5194/gmd-2020-33
Preprint. Discussion started: 27 April 2020


Geoscientific Model Development Discussions

## 2 Methods

### 2.1 Model Description

HIRM total atmospheric temperature is calculated with an IRF that characterizes the SCM's temperature response to a change in radiative forcing. This is comparable to other idealized SCMs that use IRFs as a simple way to represent major climate system dynamics (Aamaas et al., 2013; Fuglestvedt et al., 2003; Millar et al., 2017; Myhre et al., 2013). What distinguishes HIRM is that the RF input is derived from the output of a separate process-based model. This hybrid approach, combining the process-based output in an impulse response model, should be able to incorporate the nonlinear dynamics of the process-based SCM system if the majority of the nonlinear dynamics of SCMs occur between the emissions to radiative forcing calculations, and if the total atmospheric temperature is equal to the linear sum of the temperature contribution from individual radiative forcing agents.

HIRM calculates the atmospheric temperature change from preindustrial temperature ($T$) as the sum of the temperature contribution from individual forcing agents $T_i$ Eq. (1):

$$T(t) = \sum_{i=1}^{n} T_i(t), \quad (1)$$

Here the individual temperature contribution is equal to the convolution of the radiative forcing time series $RF_i$ with the temperature response to a radiative forcing pulse $IRF_i$ for a single radiative forcing agent Eq. (2).

$$T_i(t) = \int_{t_0}^{t} RF_i(t')IRF_i(t - t')dt', \quad (2)$$

The $RF_i$ and $IRF_i$ are derived from process-based climate model output. In this paper HIRM uses output from the process-based SCM Hector v 2.3.0 (Link et al. 2019) in its default release configuration. Hector is an open-source simple climate model that includes representations of the major processes driving the climate system and carbon-cycle (Hartin et al. 2015) with simple formulations rooted in the physics of ocean dynamics, atmospheric chemistry, and carbon-cycle science. Hector can be calibrated to emulate the more complex ESMs (Dorheim et al. in review) and produces realistic response to large perturbations (Schwarber et at. 2019).

### 2.2 IRF Derivation

One of Hector's assumptions is that all of Hector's radiative forcing agents exhibit the same temperature response to a change in radiative forcing. This means HIRM can be configured with a single IRF that characterizes Hector's temperature response to all of its 37 radiative forging agents. The IRF was derived using output from a reference run and a black carbon (BC) emissions perturbation run of Hector, although any forcing agent could have been selected for the perturbation run. During the reference model run Hector was driven with the RCP 4.5 scenario, while for the perturbation model run BC emissions were

https://doi.org/10.5194/gmd-2020-33
Preprint. Discussion started: 27 April 2020


Geoscientific Model Development Discussions

doubled relative to RCP 4.5 BC emissions in a single year. RCP 4.5 $CO_2$ concentrations were prescribed during these runs, suppressing Hector's normal carbon cycle temperature feedbacks.

For the purposes of the two validation experiments we did not want to include carbon-cycle climate feedbacks into the IRF, as the IRF should represent only the forcing-to-temperature response. If the $CO_2$ concentrations were allowed to change in response to carbon-climate feedbacks, the temperature response from these feedback mechanisms would be incorporated into the IRF, which would then overestimate the temperature response to the emission perturbation. For the replication experiments we focus on reproducing Hector temperature without carbon-climate feedbacks. Other applications of HIRM may require IRFs that include the temperature response from carbon-cycle feedbacks.

The emissions perturbation temperature response ($T_{response}$) was equal to the difference between the reference ($T_{ref}$) and perturbation temperature ($T_p$) Eq. (3), with the perturbation occurring at year $t_0$:

$$T_{response}(t - t_0) = T_p(t - t_0) - T_{ref}(t - t_0), \quad (3)$$

The temperature response to a radiative forcing perturbation was calculated by dividing the temperature response to the emissions perturbation by the size of the radiative forcing pulse Eq. (4). The size of the radiative forcing pulse ($X_y$) was set equal to the difference in radiative forcing between the reference and emissions perturbation runs in the perturbation year:

$$IRF_i(t - t_0) = T_{response}(t - t_0)/X_y, \quad (4)$$

The end of the IRF was extrapolated with an exponential decay function to ensure that the IRF was long enough to be convolved with HIRM's RF time series inputs without having to pad zeros onto the end or having to truncate the radiative forcing inputs.

### 2.3 Validation Experiments

#### 2.3.1 Replication of RCP Results

Emulation is used to validate HIRM by illustrating that the HIRM framework reproduces the dynamics of the process-based SCM with a minimal loss of information. If HIRM can accurately reproduce or emulate the atmospheric temperature of a more complex, process-based-model such as Hector, then HIRM's underlying assumptions about where the majority of the non-linearities occur are true. Conversely, if HIRM is unable to reproduce Hector's global temperature outputs, this would indicate that important physical and chemical processes are not being captured by the HIRM framework.

In the first validation experiment HIRM was set up to reproduce Hector temperature for RCP 2.6, RCP 4.5, RCP 6.0, and RCP 8.5. HIRM was configured each time using Hector's single IRF paired with a complete set of radiative forcing time series from Hector's 37 radiative forcing agents. The radiative forcing time series for these validation experiments came from Hector

https://doi.org/10.5194/gmd-2020-33
Preprint. Discussion started: 27 April 2020


Geoscientific Model Development Discussions

output from RCP 2.6, 4.5, 6.0, and 8.5 with prescribed $CO_2$ concentrations. For each RCP, the 37 radiative forcing time series were convolved with Hector's IRF and the result summed Eq. (1, 2). The global mean temperature outputs from Hector driven with RCP 2.6, RCP 4.5, RCP 6.0, and RCP 8.5 were saved and used as validation data for HIRM.

#### 2.3.2 Replication of 4X $CO_2$ Results

The second validation experiment tested HIRM's ability to reproduce Hector's temperature response to an abrupt four times $CO_2$ concentration step. The abrupt four times $CO_2$ concentration step is a test commonly used by climate modelers to understand the climate system's response to $CO_2$ (Schwarber et al. 2019). In this experiment HIRM was configured with Hector's IRF was paired with radiative forcing time series featuring an abrupt four times $CO_2$ concentration step test. The radiative forcing time series was obtained from Hector runs following the CMIP5 protocol (Taylor et al. 2012). HIRM's radiative forcing time series input was the difference in Hector radiative forcing from Hector driven with a constant $CO_2$ concentration of 278 ppm and Hector driven with a $CO_2$ concentration of 278 ppm until year 2010 when the $CO_2$ concentration increased by a magnitude of four and remained constant for the rest of the run. The difference in Hector's global mean temperature anomaly between the constant reference run and the perturbed step run was then compared with HIRM's output.

## 3. Results

### 3.1 Impulse Response Function

The majority of the Hector's temperature response to a radiative forcing pulse occurs within the first 50 years since the perturbation (Fig. 1). The strongest response occurs during the perturbation year itself, with a maximum value of 0.09 ($°C/W/m^2$); by year 35 the temperature response has decreased by 97% and continues to approach zero for the remainder of the IRF. This IRF is used in both of the validation experiments and case studies except where noted.

### 3.2 Validation Experiments

HIRM was able to emulate Hector's temperature for the four RCPs with a minimal loss of information (Fig. 2a). The difference between HIRM and Hector total temperature, measured as the root mean squared error (RMSE), was $1.3 \times 10^{-9}$ °C (Fig. 2a) for each RCP scenario. The cumulative percentage difference between HIRM and Hector temperature was 0.0 % (rounded from $1.0 \times 10^{-5}$; other 0.0 results are similar) for each RCP scenario. The results from this validation test confirm our first assumption: the total atmospheric temperature change is the sum of the temperature contributions from individual radiative forcing agents.

Furthermore, HIRM reproduced Hector's abrupt four times $CO_2$ concentration step temperature response with a high degree of accuracy (Fig. 2b). The RMSE between HIRM and Hector temperature output from the abrupt $CO_2$ concentration step was $1.5 \times 10^{-19}$ °C with a cumulative percent difference of 0.0%. The abrupt $CO_2$ concentration step is a standard diagnostic test

https://doi.org/10.5194/gmd-2020-33
Preprint. Discussion started: 27 April 2020


Geoscientific Model Development Discussions

used to examine climate model responses (Taylor et al. 2012; Eyring et al. 2016). Since HIRM was able to accurately emulate Hector's temperature response to a large step perturbation we conclude that the majority of the nonlinearities of the SCM are occurring during the emissions-to-radiative forcing portion of the emissions-to-temperature causal chain.

## 4 HIRM Application Case Studies

### 4.1 Aerosol Uncertainty Case Study

Uncertainties in the magnitude of historical and future radiative forcing effects continue to be a crucial challenge for climate science research, and this is particularly true for aerosol effects. In this first case study HIRM was used to explore a range of future temperature change when accounting for uncertainty in aerosol radiative forcing. To do so, HIRM was again set up to recreate Hector's RCP 4.5 temperature. In this analysis, however, the black carbon (BC), organic carbon (OC), indirect $SO_2$ effects ($SO_2$i), and direct $SO_2$ effects ($SO_2$d) RF input time series were varied. (Aerosol cloud indirect effects are represented in Hector as a function of $SO_2$ emissions only, so we refer to that as $SO_2$ indirect forcing.)

The aerosol uncertainty scalers were generated from the 2011 aerosol radiative forcing ranges reported in IPCC AR5 8.SM table 5 (Myhre et al. 2013). The BC, OC, $SO_2$i, and $SO_2$d radiative forcing IPCC ranges were individually sampled at intervals of 0.04 W/m$^2$ in 2011 (Table 1). Then default HIRM 2011 BC, OC, $SO_2$i, and $SO_2$d radiative forcing values were divided by the values sampled from the respective IPCC ranges to obtain the uncertainty scalers. HIRM was set up to run every possible combination of the scaled RF time series.

HIRM was run a total of 29,000 times creating an ensemble of uncertainty runs, these results were constrained (i.e., filtered) by historical radiative forcing and temperature. HIRM total radiative forcing were constrained to match IPCC historical estimates in radiative forcing and temperature change. The 2011 aerosol radiative forcing had to pass through the IPCC AR5 2011 aerosol uncertainty range [-1.66 to 0.14 Wm$^{-2}$] from Myhre et al. 2012. HIRM temperature trend was calculated as the slope of a linear regression and then compared to the observed temperature trend range [0.65 to 1.1] °C reported by Hartmann et al. 2013.

We found that the historical constraints had an unequal impact on the scaled radiative forcing impacts. The temperature at the end of the century for the unconstrained ensemble ranged over 2.5°C – 3.1°C; incorporating the historical constraints into the uncertainty analysis narrowed uncertainty in future temperature to 2.7°C – 2.9°C (Fig. 3). The historical constraints had different impacts on the sampled aerosol uncertainty scalers. All of the sampled OC scalers passed through the historical constraints (Fig. 4b), while the constraints had a modest effect on the OC, BC, and $SO_2$d scalers (Fig. 4a, b, and c).

https://doi.org/10.5194/gmd-2020-33
Preprint. Discussion started: 27 April 2020


Geoscientific Model Development Discussions

The historical constraints have the most noticeable effect on the $SO_2$d uncertainty scalers. This is because of the large absolute magnitude of the uncertainty in aerosol indirect effects (Myhre et al., 2013), which results in a large role for assumptions about the strength of aerosol indirect cooling. This shows that there are few numerical combinations of forcing values from other species, at least for default Hector climate system parameters, that are consistent with strong (negative) aerosol indirect forcing. The aerosol uncertainty analysis using HIRM illustrates how this modeling framework can be utilized to calculate future temperature under assumed uncertainty in aerosol radiative forcing.

### 4.1 HIRM as a Tool for Development Case Study

Radiative forcing effects from aerosols are complex (Fan et al. 2016, Bond et al. 2013), and while the physics driving these complexities have been incorporated into ESMs, they are not considered in most SCMs. For example, consider black carbon (BC): unlike cooling effects from aerosols that scatter shortwave radiation back into space, BC heats within the atmosphere, and also at the surface when deposited on snow or ice, potentially contributing to both cloud indirect cooling and heating effects (Bond et al. 2013). It can also increase cloud amounts, as BC atmospheric heating stabilizes the atmospheric thermal profile (Bond et al. 2013). Experiments conducted with ESMs have found large differences in the response to a step change in BC emissions compared to a step change in $CO_2$ (Sand et al. 2015; Yang et al. 2019).

Incorporating these dynamics into Hector would be a nontrivial task, but HIRM can be used to estimate what effect they would have on the model's global temperature. For this analysis, HIRM was set up to emulate Hector RCP 4.5 as before, but with one difference: instead of pairing the BC RCP 4.5 RF time series with Hector's single IRF, the BC RCP 4.5 RF time series was paired with a BC-specific IRF. This BC-specific IRF was derived using output from a study that performed BC emission step tests with the ESM NorESM-1 (Sand et al. 2015).

Mathematically, the derivative of a step response is equal to the impulse response function. Therefore we can derive an impulse response function from the step response results reported in the Sand et al. ESM experiment. The temperature response to a BC step in ESM experiments is well fit by a single exponential approach to a constant response (see Yang et al. 2019 for details). We fit the Sand et al. (2015) abrupt BC step response as:

$$T(t) = A\,(1 - e^{\frac{-t}{\tau}}), \tag{5}$$

The results of a nonlinear optimization of this function returned values of values of $A$ and $\tau$ that were 1.8 °C and 2.1 years, respectively. These optimal values were used in Eq. (6), the differentiated form of Eq. (5), to provide a numerical BC temperature impulse response function corresponding to the Sand et al. (2015) result:

$$\mathrm{R_t(t)} = \frac{\mathrm{A}}{\tau}\,\mathrm{e}^{\frac{-\mathrm{y}}{\mathrm{t}}}\mathrm{dt}, \tag{6}$$

https://doi.org/10.5194/gmd-2020-33
Preprint. Discussion started: 27 April 2020


Geoscientific Model Development Discussions

The numerical result of Eq. (6) is converted to a BC impulse response per unit forcing by dividing by the forcing from a 133 Tg BC emissions change (used in Sand et al. 2015) using Hector's default forcing per unit BC emission assumptions. With this transformation we have replaced Hectors' default BC representation in HIRM with the Sand et al. temperature response in both magnitude and temporal behavior.

We found that the BC Sand et al. IRF has a weaker temperature response in the perturbation year and a more rapid decline in temperature response compared to Hector's global IRF (Fig. 5a). The maximum IRF response for the BC Sand et al. IRF is 0.06 ($°C/W/m^2$) which is 0.03 ($°C/W/m^2$) cooler than Hector's IRF. In addition, the BC. Sand et al. IRF approaches 0 ($°C/W/m^2$) faster than Hector's IRF. These differences are expected since the BC Sand et al. IRF was derived from the NorESM-1 ESM, meaning that this IRF incorporates the complex cooling and warming effects of BC emissions, the net warming over land as compared to no net warming over oceans (Sand et al. 2015). When HIRM was configured with the BC Sand et al. (2015) IRF the global temperature decreased by 0.2 °C from 1750 to 2100 under the RCP 4.5 scenario (Fig. 5b). Based on these results, if Hector were modified to emulate this BC response we predict that the model's global temperature would be cooler by approximately 0.2 °C in 2100.

## 5 Discussion and Conclusion

In this paper we document and test HIRM, a framework that leverages the nonlinear dynamics of process-based SCMs within a computationally efficient, highly idealized linear impulse response model. The HIRM framework can be used as a testbed to quickly examine the consequences of different model assumptions, as demonstrated by the two case studies. Furthermore, we can draw conclusions about process-based climate models such as Hector (Hartin et al. 2015) based on HIRM. While other IRFs have incorporated nonlinear dynamics using nonlinear terms (Hooß et al. 2001, Millar et al. 2017), HIRM is distinguished by its lack of nonlinear terms, but it nonetheless demonstrates nonlinear dynamics because the majority of the nonlinear dynamics are incorporated into the forcing time series that drives HIRM. HIRM is available as an open source R package (available at https://github.com/JGCRI/HIRM), its computational flexibility and short run time make is particularly appropriate for uncertainty analyses and experimental SCM design.

We demonstrated that HIRM can be used to examine uncertainty within the climate system, and that incorporating a more realistic BC temperature response dynamics into Hector has a significant impact on Hector's global temperature. If more studies corroborate the findings of Sand et al. (2015) and Yang et al. (2019) by observing shorter timescale responses for BC temperature dynamics across a number of ESMs and Atmosphere-Ocean General Circulation Models (AOGCMs), then SCM modeling groups will need to consider incorporating the BC temperature response dynamics into SCMs. Some SCMs, such as MAGICC 5.3 and MAGICC 6 (Wigely et al. 2002), already exhibit multiple temperate responses; interestingly, MAGICC has

https://doi.org/10.5194/gmd-2020-33
Preprint. Discussion started: 27 April 2020


a shorter timescale for the temperature response for aerosols (Schwarber et al. 2019), but the resulting response in MAGICC still has a longer timescale than that from the AOGCMs (Sand et al. 2015, Yang et al. 2019).

During the HRIM validation experiments we found that most of non-linearities are in the emissions to forcing step, in which the SCM calculates concentrations from emissions and radiative forcings from concentrations. This implies that efforts to improve the representation of nonlinear behavior in SCMs should be focused on this emissions-to-forcing step. We note that we draw this conclusion by calibrating HIRM to a single process-based SCM; this finding should be verified using other models, including Earth System Models of Intermediate Complexity (Claussen et al. 2002). Such EMICs have more physically-based parameterizations but low levels of internal model noise, which would be valuable for such explorations. If this finding holds for a wider class of models, this would mean that a wide range of model responses to forcing could be quickly simulated using IRFs. Good et al. 2013 showed that SCMs based on step responses work fairly well for more reproducing General Circulation Model (GCM) results suggesting that the assumptions underlying HIRM are valid.

One limitation of this framework is that interactions between forcing agents are not directly considered. For example, multiple species of aerosols may contribute to cloud indirect cooling effects. These interactions, however, are not well constrained (Fan et al. 2016) and, for many purposes where SCMs might be applicable, it is most important to be able to represent the overall (large) uncertainty range, rather than interactions among species that have yet to be definitively quantified. An effort to represent aerosol indirect effects semi-analytically (Ghan et al. 2013) demonstrated not only the multiple processes that are relevant but also the difficulty in understanding the drivers of the different forcing estimates from more complex models.

While impulse response functions have been used widely in the scientific community, they have well-known limitations. At least in the context of the SCM used here, we demonstrate that the use of a forcing-based impulse response function overcomes most of these limitations. This insight should be useful in future work applying impulse response functions in general and the design of simple climate models in particular. These findings imply that improvements to simple climate models should focus on improving the representation of emission to concentration and concentration to forcing relationships. As we note above, however, it would be useful to also design comparisons with more complex models, perhaps EMICS given their lower noise and computational requirements, to determine the extent to which the temperature response to forcing in more complex models can be accurately represented by impulse response functions, particularly on 20-30 year time scales where GCM outputs are particularly noisy.

While the application of HIRM in this work was facilitated by the presence of an existing R-based interface with the Hector simple climate model, HRIM could also be used with data generated by other SCMs. This could be a useful way of decomposing differences in responses between SCMs (e.g. Nicholls et al. 2020) into differences in the emissions to forcing

https://doi.org/10.5194/gmd-2020-33
Preprint. Discussion started: 27 April 2020


Geoscientific Model Development Discussions

step compared to differences in the model's response to a forcing impulse. Similarly, HIRM could be used to examine the uncertainty due to the different forcing to temperature responses amongst SCMs.

HIRM can be used as a testbed for future SCM development. As demonstrated here, the incorporation of a GCM-derived temperature response function for black carbon emissions results in a significantly different global mean temperature response (Figure 5). Exploration of the potential impact of such changes can be done quickly in HIRM to decide if changes should be incorporated into, for example, Hector. Incorporating such a change into the Hector model itself would be a more time and labor intensive process for several reasons. First, to incorporate this change into Hector one would need to decide how to physically interpret the faster BC response time seen in GCMs since Hector does not use impulse response functions directly. There is some debate if this is due to different response over land vs ocean, or if this is more closely related to differing hemispheric responses (Meinshausen et al. 2011, Shindell 2014, Sand et al. 2015). Further, explorations or model extensions using HIRM can be accomplished without a user having to understand Hector's code, dependencies, and coding standards.

Finally, this framework could also be used for analysis that requires capabilities not present in SCMs–for example, regional analysis. Regional temperature trends could be simulated by HRIM by incorporating the ratio of regional to global temperature responses for each forcing agent into HIRM (Sand et al. 2019 and Shindell and Faluvegi et al. 2009). This could be particularly valuable for a region such as the Arctic, where a variety of forcing agents, from regional sulfate (Acosta Navarro et al. 2016), local black carbon (Sand et al. 2013 and Yang et al. 2019), and global forcing changes, e.g. Arctic amplification, all may play a role. This type of analysis could readily be accomplished using HRIM, including the wide range of uncertainty space that should be examined (e.g. Figure 3).

## Code availability

HIRM as an R package is available at https://github.com/JGCRI/HIRM with an online manual available at https://jgcri.github.io/HIRM/ . The package is archived on Zenodo (https://doi.org/10.5281/zenodo.3756122), however because of Zenodo storage limits the code and results related to the discussion and conclusions of this paper are available on the Open Science Framework (OSF) at https://osf.io/kmrj8/.

## Author contributions

S. Smith conceptualized the Hybrid Impulse Response Model (HIRM). K. Dorheim and B. P. Bond-Lamberty developed the project software. K. Dorheim wrote the manuscript with contributions from all co-authors.

https://doi.org/10.5194/gmd-2020-33
Preprint. Discussion started: 27 April 2020


Geoscientific Model Development Discussions

## Competing interests

The authors declare that they have no conflict of interest.

## Acknowledgements

We thank Robert Link for invaluable insight regarding HIRM development as an R package and M. Sand for numerical model results. This research was supported by the United States Environmental Protection Agency.

https://doi.org/10.5194/gmd-2020-33
Preprint. Discussion started: 27 April 2020




**References**

Aamaas, B., G. P. Peters, and J. S. Fuglestvedt. "Simple Emission Metrics for Climate Impacts." Earth Syst. Dynam. 4, no. 1 (June 6, 2013): 145–70. https://doi.org/10.5194/esd-4-145-2013.

Bond, T. C., S. J. Doherty, D. W. Fahey, P. M. Forster, T. Berntsen, B. J. DeAngelo, M. G. Flanner, et al. "Bounding the Role of Black Carbon in the Climate System: A Scientific Assessment." Journal of Geophysical Research: Atmospheres 118, no. 11 (June 16, 2013): 5380–5552. https://doi.org/10.1002/jgrd.50171.

Caldeira, K, and N P Myhrvold. "Projections of the Pace of Warming Following an Abrupt Increase in Atmospheric Carbon Dioxide Concentration." Environmental Research Letters 8, no. 3 (September 2013): 034039. https://doi.org/10.1088/1748-9326/8/3/034039.

Claussen, M., L. Mysak, A. Weaver, M. Crucifix, T. Fichefet, M.-F. Loutre, S. Weber, et al. "Earth System Models of Intermediate Complexity: Closing the Gap in the Spectrum of Climate System Models." Climate Dynamics 18, no. 7 (March 1, 2002): 579–86. https://doi.org/10.1007/s00382-001-0200-1.

Dorheim, Kalyn, Robert Link, Corinne Hartin, Ben Kravitz, and Abigail Snyder. "Calibrating Simple Climate Models to Individual Earth System Models: Lessons Learned from Calibrating Hector." Under Review in Earth and Space Science, n.d.

Eyring, V., S. Bony, G. A. Meehl, C. A. Senior, B. Stevens, R. J. Stouffer, and K. E. Taylor. "Overview of the Coupled Model Intercomparison Project Phase 6 (CMIP6) Experimental Design and Organization." Geosci. Model Dev. 9, no. 5 (May 26, 2016): 1937–58. https://doi.org/10.5194/gmd-9-1937-2016.

Fan, Jiwen, Yuan Wang, Daniel Rosenfeld, and Xiaohong Liu. "Review of Aerosol–Cloud Interactions: Mechanisms, Significance, and Challenges." Journal of the Atmospheric Sciences 73, no. 11 (July 11, 2016): 4221–52. https://doi.org/10.1175/JAS-D-16-0037.1.

Good, Peter, Jonathan M. Gregory, Jason A. Lowe, and Timothy Andrews. "Abrupt CO2 Experiments as Tools for Predicting and Understanding CMIP5 Representative Concentration Pathway Projections." Climate Dynamics 40, no. 3 (February 1, 2013): 1041–53. https://doi.org/10.1007/s00382-012-1410-4.

Hartin, Corrine, Pralit Patel, Adria Schwarber, Robert Link, and Ben Bond-Lamberty. "A Simple Object-Oriented and Open-Source Model for Scientific and Policy Analyses of the Global Climate System–Hector v1. 0." Geoscientific Model Development, April 1, 2015, 939–55. https://doi.org/doi:10.5194/gmd-8-939-2015.

Hooss, G., R. Voss, K. Hasselmann, E. Maier-Reimer, and F. Joos. "A Nonlinear Impulse Response Model of the Coupled Carbon Cycle-Climate System (NICCS)." Climate Dynamics 18, no. 3 (December 1, 2001): 189–202. https://doi.org/10.1007/s003820100170.

https://doi.org/10.5194/gmd-2020-33
Preprint. Discussion started: 27 April 2020




Houghton, John T., L. Gylvan Meira Filho, David J. Griggs, and Kathy Maskell. An Introduction to Simple Climate Models Used in the IPCC Second Assessment Report. WMO, 1997.

Hurrell, James W., M. M. Holland, P. R. Gent, S. Ghan, Jennifer E. Kay, P. J. Kushner, J.-F. Lamarque, et al. "The Community Earth System Model: A Framework for Collaborative Research." Bulletin of the American Meteorological Society 94, no. 9 (2013): 1339–60. https://doi.org/10.1175/BAMS-D-12-00121.1.

Intergovernmental Panel on Climate Change, ed. "Observations: Atmosphere and Surface." In Climate Change 2013 – The Physical Science Basis: Working Group I Contribution to the Fifth Assessment Report of the Intergovernmental Panel on Climate Change, 159–254. Cambridge: Cambridge University Press, 2014. https://doi.org/10.1017/CBO9781107415324.008.

Joos, F., R. Roth, J. S. Fuglestvedt, G. P. Peters, I. G. Enting, W. von Bloh, V. Brovkin, et al. "Carbon Dioxide and Climate Impulse Response Functions for the Computation of Greenhouse Gas Metrics: A Multi-Model Analysis." Atmos. Chem. Phys. 13, no. 5 (March 8, 2013): 2793–2825. https://doi.org/10.5194/acp-13-2793-2013.

Kriegler, Elmar. "Imprecise Probability Analysis for Integrated Assessment of Climate Change." Verlag nicht ermittelbar, 2005.

Link, Robert, Ben Bond-Lamberty, Corinne Hartin, Alexey Shiklomanov, bvegawe, Pralit Patel, Sven Willner, et al. JGCRI/Hector: Hector Version 2.3.0 (version v2.3.0). Zenodo, 2019. https://doi.org/10.5281/zenodo.3144007.

Meinshausen, M, S.C.B. Raper, and T.M.L. Wigley. "Emulating Coupled Atmosphere-Ocean and Carbon Cycle Models with a Simpler Model, MAGICC6 – Part 1: Model Description and Calibration." Atmos. Chem. Phys. 11 (2011): 1417–1456. https://doi.org/10.5194/acp-11-1417-2011.

Millar, R. J., Z. R. Nicholls, P. Friedlingstein, and M. R. Allen. "A Modified Impulse-Response Representation of the Global near-Surface Air Temperature and Atmospheric Concentration Response to Carbon Dioxide Emissions." Atmos. Chem. Phys. 17, no. 11 (June 16, 2017): 7213–28. https://doi.org/10.5194/acp-17-7213-2017.

Myhre, G., D. Shindell, F.M. Breon, W. Collins, J. Fuglestvedt, and J. Huang. "Anthropogenic and Natural Radiative Forcing." In Climate Change 2013: The Physical Science Basis. Contribution of Working Group I to the Fifth Assessment Report of the Intergovernmental Panel on Climate Change. Cambridge University Press, 2013.

Nicholls, Z. R. J., M. Meinshausen, J. Lewis, R. Gieseke, D. Dommenget, K. Dorheim, C.-S. Fan, et al. "Reduced Complexity Model Intercomparison Project Phase 1: Protocol, Results and Initial Observations." Geoscientific Model Development Discussions 2020 (2020): 1–33. .

Pincus, R., P. M. Forster, and B. Stevens. "The Radiative Forcing Model Intercomparison Project (RFMIP): Experimental Protocol for CMIP6." Geoscientific Model Development 9, no. 9 (2016): 3447–3460.

https://doi.org/10.5194/gmd-2020-33
Preprint. Discussion started: 27 April 2020


Sand, M., T. Iversen, P. Bohlinger, A. Kirkevåg, I. Seierstad, Ø. Seland, and A. Sorteberg. "A Standardized Global Climate Model Study Showing Unique Properties for the Climate Response to Black Carbon Aerosols." Journal of Climate 28, no. 6 (January 8, 2015): 2512–26. https://doi.org/10.1175/JCLI-D-14-00050.1.

Schwarber, Adria K., Steven J. Smith, Corinne A. Hartin, Benjamin Aaron Vega-Westhoff, and Ryan Sriver. "Evaluating Climate Emulation: Unit Testing of Simple Climate Models." Earth System Dynamics Discussions, 2019, 1–13.

Sherwood, Steven C., Sandrine Bony, Olivier Boucher, Chris Bretherton, Piers M. Forster, Jonathan M. Gregory, and Bjorn Stevens. "Adjustments in the Forcing-Feedback Framework for Understanding Climate Change." Bulletin of the American Meteorological Society 96, no. 2 (2015): 217–28. https://doi.org/10.1175/BAMS-D-13-00167.1.

Smith, C. J., R. J. Kramer, G. Myhre, P. M. Forster, B. J. Soden, T. Andrews, O. Boucher, et al. "Understanding Rapid Adjustments to Diverse Forcing Agents." Geophysical Research Letters 45, no. 21 (2018): 12,023-12,031. https://doi.org/10.1029/2018GL079826.

Solomon, S., D. Qin, M. Manning, Z. Chen, M. Marquis, K. Averyt, M. Tignor, and H. Miller. "IPCC Fourth Assessment Report (AR4)." Climate Change, 2007.

Stainforth, D. A., T. Aina, C. Christensen, M. Collins, N. Faull, D. J. Frame, J. A. Kettleborough, et al. "Uncertainty in Predictions of the Climate Response to Rising Levels of Greenhouse Gases." Nature 433, no. 7024 (January 1, 2005): 403–6. https://doi.org/10.1038/nature03301.

Stjern, Camilla Weum, Marianne Tronstad Lund, Bjørn Hallvard Samset, Gunnar Myhre, Piers M. Forster, Timothy Andrews, Olivier Boucher, et al. "Arctic Amplification Response to Individual Climate Drivers." Journal of Geophysical Research: Atmospheres 0, no. ja (n.d.). https://doi.org/10.1029/2018JD029726.

Strassmann, K.M., and F. Joos. "The Bern Simple Climate Model (BernSCM) v1.0: An Extensible and Fully Documented Open-Source Re-Implementation of the Bern Reduced-from Model for Global Carbon Cycle-Climate Simulations." Geoscientific Model Development 11 (2018): 1887–1908.

Thompson, Matthew V., and James T. Randerson. "Impulse Response Functions of Terrestrial Carbon Cycle Models: Method and Application." Global Change Biology 5, no. 4 (April 1, 1999): 371–94. https://doi.org/10.1046/j.1365-2486.1999.00235.x.

Vuuren, Detlef va, Jason Lowe, Elke Stehfest, Laila Gohar, Andries Hof, Chris Hope, Rachel Warren, Malte Meinshausen, and Gian-Kasper Plattner. "How Well Do Integrated Assessment Models Imulate Cliamte Change?" Climatic Change 104 (2011): 255–85. https://doi.org/10.1007/s10584-009-9764-2.

Webster, Mort, Andrei P. Sokolov, John M. Reilly, Chris E. Forest, Sergey Paltsev, Adam Schlosser, Chien Wang, et al. "Analysis of Climate Policy Targets under Uncertainty." Climatic Change 112, no. 3 (June 1, 2012): 569–83. https://doi.org/10.1007/s10584-011-0260-0.

https://doi.org/10.5194/gmd-2020-33
Preprint. Discussion started: 27 April 2020


Geoscientific Model Development Discussions

410

| RF agent | Min. 2011 RF | Max. 2011 RF | Hector Default 2011 RF |
|---|---|---|---|
| **BC** | 0.05 | 0.87 | 0.40 |
| **OC** | -0.21 | -0.04 | -0.17 |
| **$SO_2i$** | -1.2 | 0 | -0.60 |
| **$SO_2d$** | -0.6 | -0.2 | -0.35 |

**Table 1: The minimum and maximum 2011 radiative forcing values from IPCC AR5 8.SM table 5 (Myhre et al. 2013). These values were used to obtain the min and max aerosol uncertainty scalers for four RF agents (BC, OC, $SO_2i$, and $SO_2d$). Along with the 2011 RF of the default configuration of HIRM/Hector for RCP 4.5.**

415

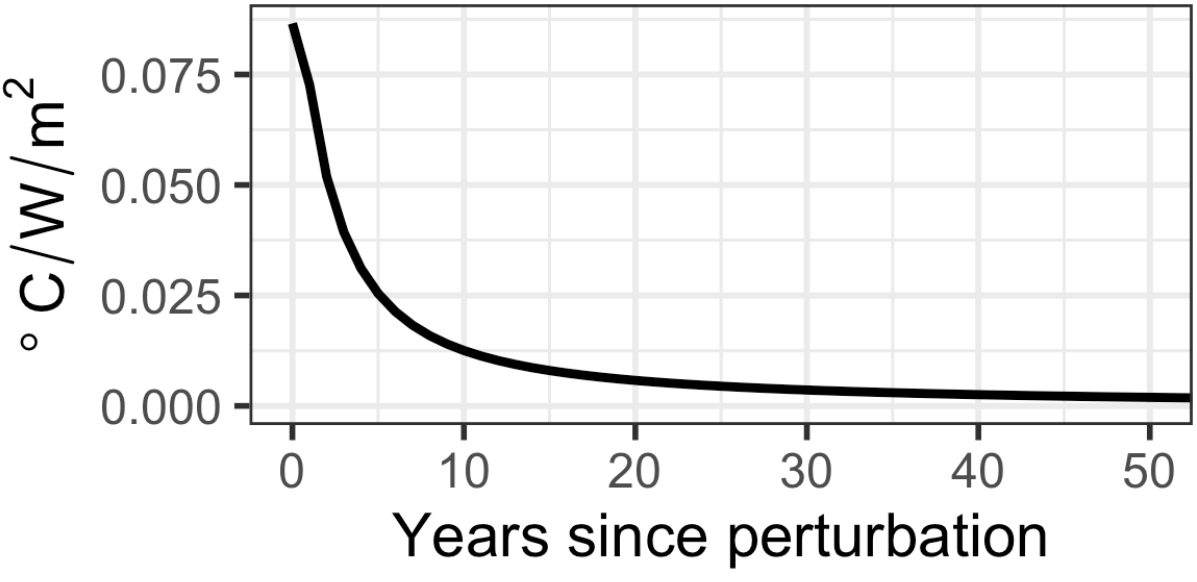

https://doi.org/10.5194/gmd-2020-33
Preprint. Discussion started: 27 April 2020


Geoscientific Model Development Discussions

**Figure 1: The first 50 years of the global temperature response to a radiative forcing perturbation for Hector v2.0; the remaining 2,500 years of the impulse response are almost constant and slowly approach zero. Here the black carbon emissions were doubled in 2010 relative to the Representative Concentration Pathway 4.5 value.**

https://doi.org/10.5194/gmd-2020-33
Preprint. Discussion started: 27 April 2020


Geoscientific Model Development Discussions

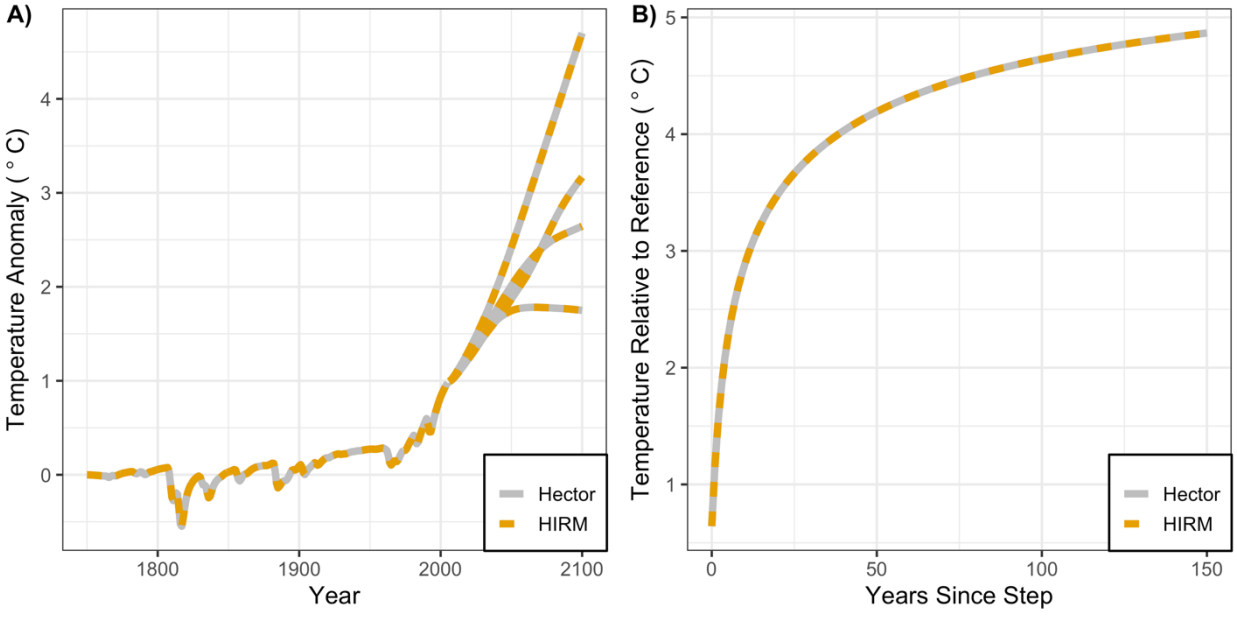


425

**Figure 2: Comparison of Hector (grey dashed) and HIRM (orange dashed) global mean temperature anomaly from the two validation experiments. In panel (A) HIRM was used to the recreate Hector temperature for the four RCPs. The four lines in panel (A) from lowest to highest 2100 temperature represent results for RCP 2.6, RCP 4.5, RCP 6.0 and RCP 8.5. Panel (B) compares the temperature response of HIRM and Hector from the abrupt four times $CO_2$ concentration step validation test.**

430

https://doi.org/10.5194/gmd-2020-33
Preprint. Discussion started: 27 April 2020


Geoscientific Model Development Discussions

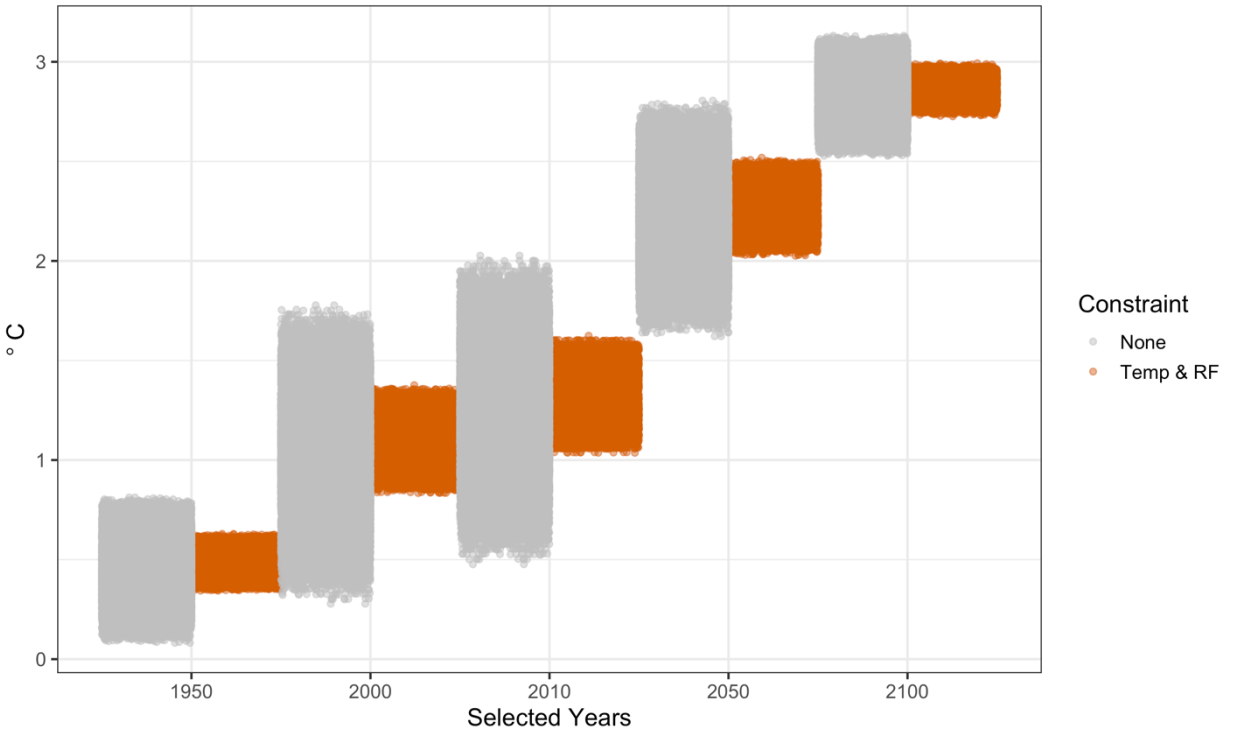


**Figure 3: The temperature (°C)_spread from the aerosol uncertainty runs in selected years. The grey regions show all of the possible runs before the historical constraints were put into the place; orange regions are the runs that passed through both historical temperature and radiative forcing constraints.**

https://doi.org/10.5194/gmd-2020-33
Preprint. Discussion started: 27 April 2020


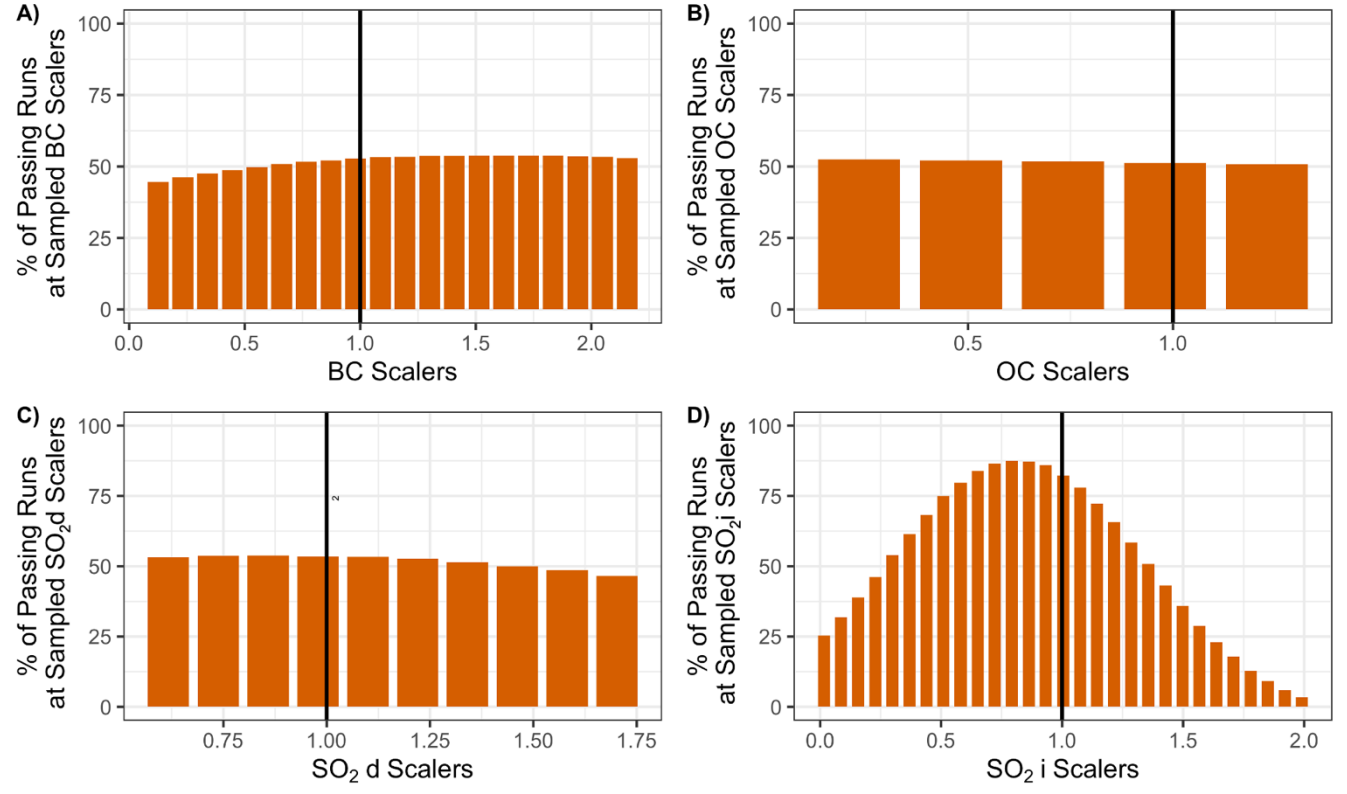


**Figure 4: Uncertainty scalers used to vary (A) black carbon, (B) organic carbon, (C) direct $SO_2$ effects, and (D) indirect $SO_2$ effects aerosol RF time series in the uncertainty analysis. HIRM was run a total of 29,000 with every combination of uncertainty scaler represented on the x-axes of panels A-D, creating an ensemble of uncertainty runs with scalars varying for all radiative forcing agents. Each panel of this figure plots a projection of the percent of runs passing through the historical constraints for one radiative forcing agent as the uncertainty scaler is varied. The black vertical line marks the 1.0 scaler; scalers larger than 1 will enhance the radiative forcing agent effects relative to the default value, while those less than 1.0 decrease the effects.**

https://doi.org/10.5194/gmd-2020-33
Preprint. Discussion started: 27 April 2020


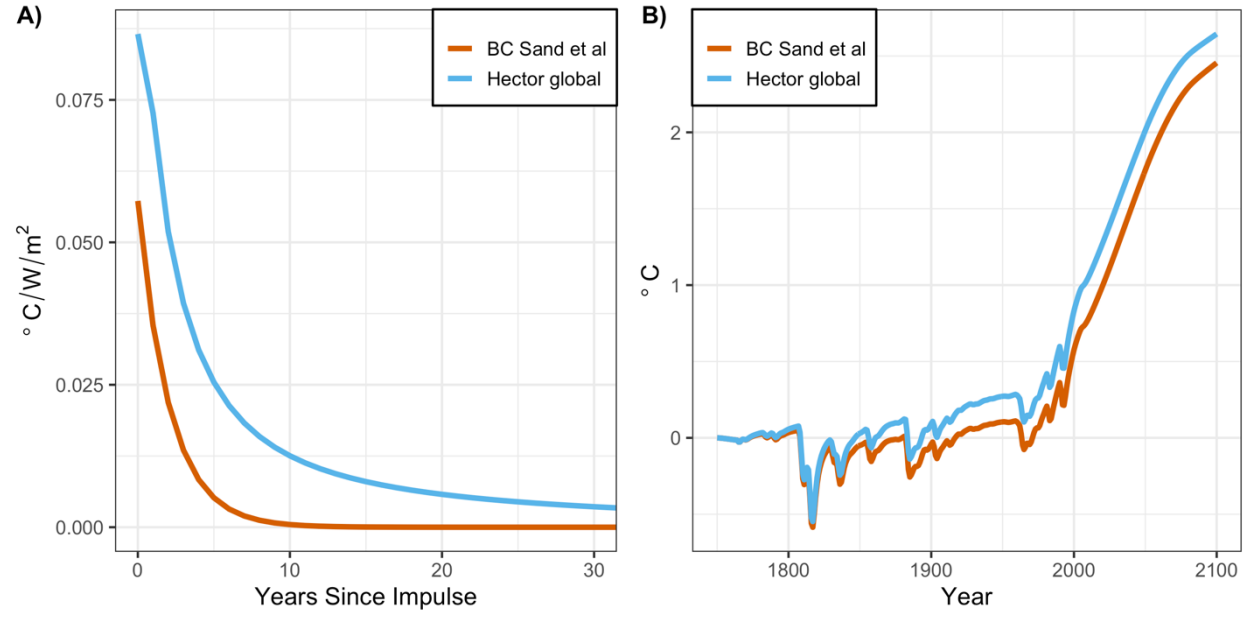


**Figure 5: (A) Hector's IRF (blue) compared with the BC Sand et al. 2015 IRF (red). (B) HIRM total temperature for the Representative Concentration Pathway 4.5 for two HIRM cases, one that only uses Hector's IRF (blue) and the other pairing the BC RF time series with the BC Sand et al. 2015 IRF (red).**